Research Article

Grid-secluded Induction Generator with ANN and Interval Type-2 Fuzzy based Controller for Wind Power Generation with Smart Load Control

Arunava Chatterjee[1], Bratati Banerjee[2]

1. Electrical Engineering Department, Raghunathpur Government Polytechnic, Sultandi, India; 2. University of Burdwan, India

Three-phase Induction generators are widely used to extract power from wind both in grid-connected and isolated conditions. This paper proposes an induction generator-based generation scheme with innovative power point tracking capability for standalone operation. The scheme is suitable for use in remote and grid inaccessible areas as a means of extracting electric power from wind. An inverter connected across the generator acts as a source of variable excitation and regulates the load voltage during changing loads or low wind speed conditions. The obtained power is converted to DC and the same is again fed to loads via a three-phase inverter run at a fixed frequency. Optimal power generation is ensured using an artificial neural network (ANN) and an interval Type-2 Fuzzy inference system enabled maximum power point tracking (MPPT)-based controller. For the wind turbine system, ANN is used to estimate the maximum output voltage value and interval type-2 fuzzy logic is used for the generation of optimum duty cycle for pulses of the converter. A smart load controller is correspondingly proposed based on ANN which can consistently isolate loads with incipient faults. The novelty of the scheme lies in the ease of implementation, proposal of a new MPPT strategy with smart load control. Appropriate simulation and experimental results validate the proposed strategy, along with suitable comparisons.

Corresponding authors: Arunava Chatterjee, arunava7.ju@gmail.com; Bratati Banerjee, bratati.biochem@gmail.com

 doi.org/10.32388/D4GAVP.2

I. Introduction

With increase in global energy demand and with increase in fossil fuel costs, the use of renewable sources of energy like wind power has become crucial. In a developing country like India, remote and countryside electrification is difficult to establish, especially due to economic considerations of high cost of transmission lines and associated losses. Therefore, a suitable standalone renewable source of generation can be used in microgeneration-based applications to supply remote and grid inaccessible loads. Among renewable energy sources, wind is a confined, copious, and clean energy source but with an intermittent nature and hence uncontrollable [1]. Obtaining a stable source of power from a wind energy generation system is thus challenging. Induction generators are extensively used in association with wind turbines for generation of electricity in grid connected as well as small-scale standalone purposes [2][3][4][5][6]. An induction machine has some inherent advantages of low cost, robustness, almost maintenance free and no requirement of DC excitation. Self-excited, induction generators almost always suffer from the problem of voltage regulation as the output voltage is dependent on the terminal connected capacitors [4]. With increase in load, the induction generator's requirement for reactive power increases. Modified inverter assisted control scheme proposed previously aims to increase the operating range of the generator [7], [8]. However, the issue of load voltage collapse may arise if load current increase, as a single battery may drain out with an increase in load. A suitable closed loop scheme with backup power is thus necessary. Load controllers were used previously to keep the output power constant with variable terminal loads [9]. These controllers use a specially designed dump load sometimes along with DC link capacitor which increases the overall outlay of the system. The three-phase standalone induction generators can also suffer faults especially inter-turn faults and can be a serious problem when they are operated in standalone mode [10]. While grid connected generation are easier to control via MPPT techniques [11][12][13], standalone grid-secluded generations are often controlled without MPPT to avoid complexity. However, since standalone generations are often used to cater to critical loads [14], [15] maintaining a steady generation becomes essential.

In this paper, a three-phase, cage rotor induction machine is used as an induction generator which is driven by a wind-turbine with artificial neural network (ANN) and interval type-2 fuzzy inference based MPPT control for the wind generation. The employed controller is easy to implement the modelling complexity of voltage availability. Besides, using interval type-2 fuzzy inference can extensively be applied in rule-based fuzzy logic systems for modelling uncertain systems like availability of wind

power. The loads are controlled using a smart ANN based controller and it has the feature to isolate loads with incipient faults. A bulk capacitor is connected across the stator winding terminals to provide excitation during initial generation. The bidirectional converter assembly connected across the terminals consists of a three-phase pulse width modulated PWM inverter for providing the variable excitation. When load increases or alternatively, when the wind power becomes low, the converter provides the necessary additional excitation to maintain the induction generator magnetic field, thereby keeping the real power constant at load terminals. The major takeaways from the proposed generation scheme are:

- An MPPT controller is proposed based on ANN and interval type-2 fuzzy inference-based control. The control is unique with comparatively easier implementation and use.
- A smart ANN based load control is proposed which is capable to determine loads having incipient faults. The loads can be isolated for further inspection.
- Short-time voltage oscillations are also minimized with the proposed control.

The experimental and simulation results justify the suitability of the concept for remote and grid isolated purposes. The paper is organized as follows: Section II proposes the generation scheme and its model. Section III details the adopted control procedures. Simulation and experimental results are provided in Section IV and finally Section V draws the conclusion and proposes the future scope of the study.

II. Proposed Generation Scheme and its Modelling

A three-phase, cage rotor induction machine is used as the induction generator. The induction machine's stator winding terminals are connected to a capacitor of suitable value which will provide the initial VAr required for generation at nominal cut-off speed and no-load conditions. As the machine starts to generate, loads can be connected across the stator winding terminals across the terminal capacitor. However, the maintenance for fixed frequency is assured by using a three-phase fixed frequency inverter connected at the load side. The generator side converter is essentially a three-phase inverter operating in bidirectional mode with its DC bus connected to a capacitor. The load side inverter frequency is maintained at constant 50Hz using a microcontroller which generates the gating pulses for the inverter switches. Provision for storage of this energy is kept by a storage battery connected across the bus. The bidirectional converter along with the storage battery constituting the converter assembly will provide the necessary variable excitation during an increase in terminal electrical load or during low rotor speeds. The setup for the proposed generation scheme is shown in Fig.1.

The load voltage is kept steady using a closed loop voltage controller to control the inverter output using artificial neural network (ANN) with interval type-2 fuzzy based controller. The load voltage is compared with a reference voltage and is fed to a proportional-integral (PI) controller. The output is fed to gate driver to generate the PWM pulses. If the wind speed increases or load decreases, the surplus power generated by the generator gets stored in the storage battery. The induction generator is modeled using the generalized *d*-*q*-axes machine model in synchronously rotating reference frame having speed ω_e [16],

$$v_{ds} = R_{ds} i_{ds} + \frac{d}{dt}\psi_{ds} - \omega_e \psi_{qs} \qquad (1)$$

$$v_{qs} = R_{qs} i_{qs} + \frac{d}{dt}\psi_{qs} + \omega_e \psi_{ds} \qquad (2)$$

$$0 = R_{dr} i_{dr} + \frac{d}{dt}\psi_{dr} - (\omega_e - \omega_r)\psi_{qr} \qquad (3)$$

$$0 = R_{qr} i_{qr} + \frac{d}{dt}\psi_{qr} + (\omega_e - \omega_r)\psi_{dr} \qquad (4)$$

where, R_{ds}, R_{qs}, are the respectively the *d* and *q* axis stator resistances, v_{ds}, v_{qs} are the *d*-*q*-axis stator voltages, i_{ds}, i_{qs}, i_{dr} and i_{qr} are the stator and rotor *d*-axis and *q*-axis currents respectively. ω_r is the speed of the rotor. Flux relations [16] are,

$$\psi_{ds} = L_{lds} i_{ds} + L_{dm}(i_{ds} + i_{dr}) \qquad (5)$$

$$\psi_{qs} = L_{lqs} i_{qs} + L_{qm}(i_{qs} + i_{qr}) \qquad (6)$$

$$\psi_{dr} = L_{ldr} i_{dr} + L_{dm}(i_{ds} + i_{dr}) \qquad (7)$$

$$\psi_{qr} = L_{lqr} i_{qr} + L_{qm}(i_{qs} + i_{qr}) \qquad (8)$$

ψ_{ds}, ψ_{qs}, ψ_{dr} and ψ_{qr} are the stator *d*-axis, *q*-axis and rotor *d*-axis, *q*-axis flux linkages respectively, L_{lds}, L_{lqs}, L_{ldr} and L_{lqr} are the stator *d*-axis, *q*-axis and rotor *d*-axis, *q*-axis leakage inductances. L_{dm} and L_{qm} are the magnetizing inductances of d and q axes respectively.

Now, when an *R*-*L* load is connected across the generator windings,

$$C\frac{d}{dt}v_{qs} = -(i_{qs} - i_{ql}) \qquad (9)$$

$$v_{qs} = R_l i_{ql} + L_l \frac{d}{dt} i_{ql} + \omega_e L_l i_{dl} \qquad (10)$$

where, R_l, L_l, i_{ql}, i_{dl} and *C* are the load resistance, load inductance, *q* and *d* axes load currents and the terminal capacitor respectively. The inverter voltage equation can be given as,

$$v_{ds} = s_{fn}.v_{dc} \qquad (11)$$

where, v_{dc} is the voltage of the storage battery and S_{fn} is the inverter switching function. Accordingly, the induction generator equivalent circuit can be formed using the abovementioned equations in d-q axes synchronously rotating reference frame. Fig.2. shows the equivalent circuit of the induction generator in d-q axes synchronously rotating reference frame as obtained from the above equations. Fig.2(a) is the d-axis equivalent circuit whereas Fig.2(b) is the q-axis equivalent circuit.

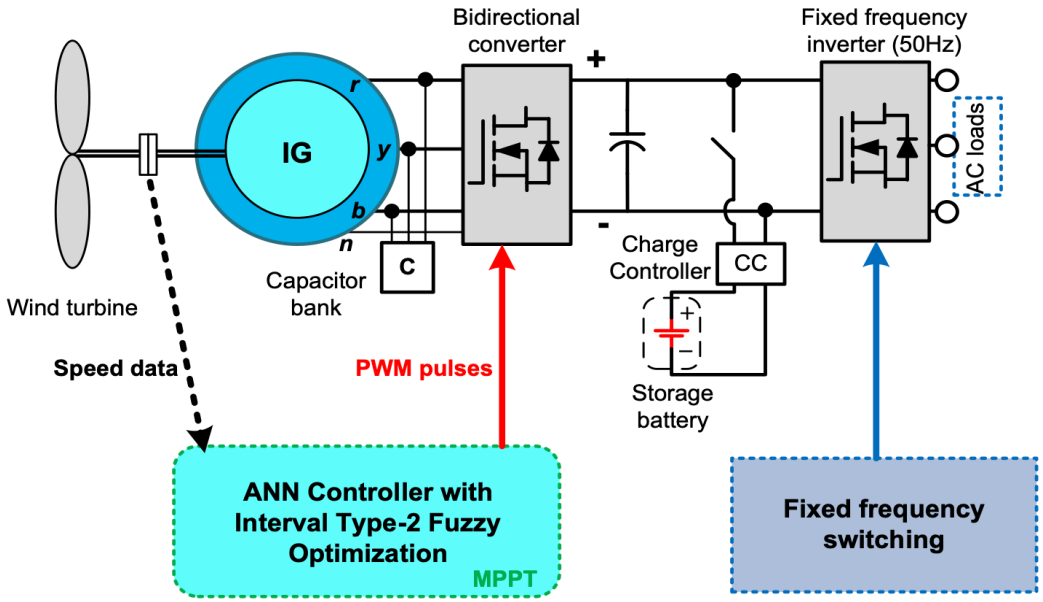

Fig.1. Setup for the proposed generation scheme.

doi.org/10.32388/D4GAVP.2

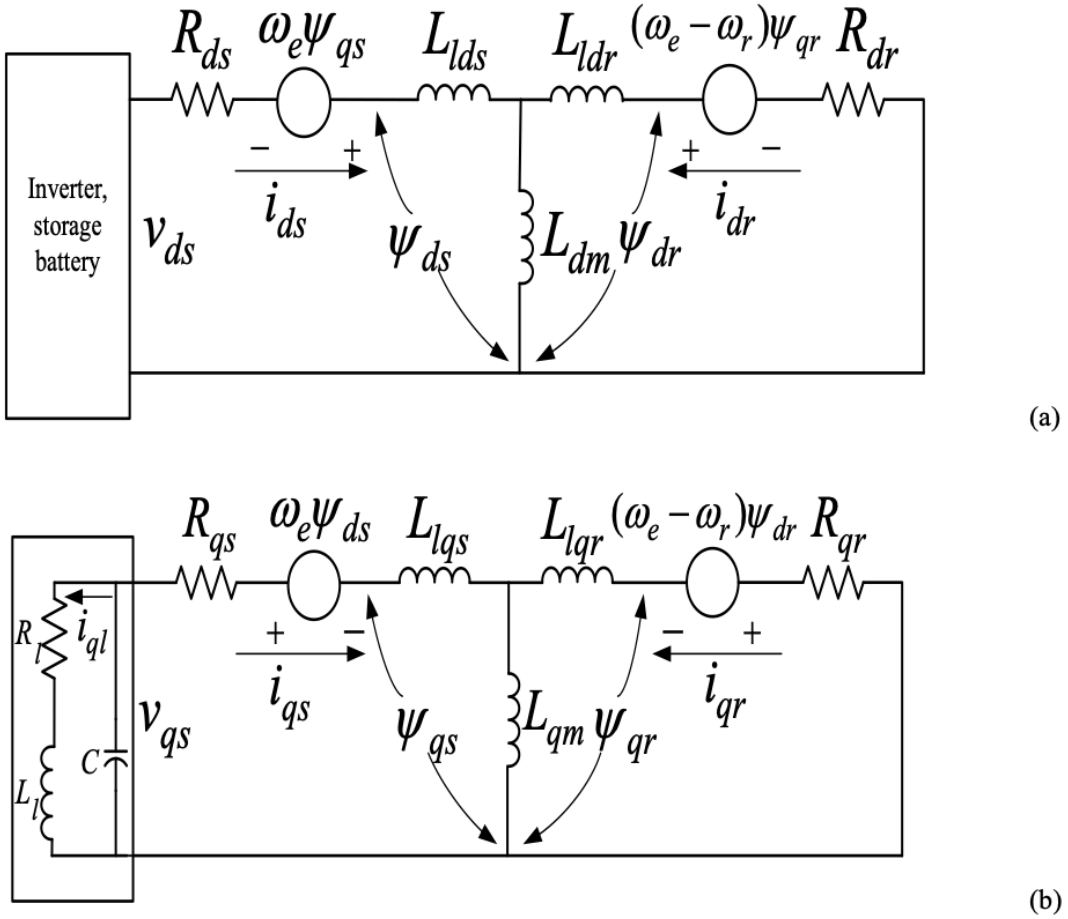

Fig.2. Induction generator (a) *d*-axis and (b) *q*-axis equivalent circuit.

ANN is a computational model inspired by the structure and working of the human brain [17]. It has also been used for improvement of performance from wind energy conversion systems as in [18], [19]. It is a type of machine learning algorithm that can be trained to recognize patterns in data and make predictions based on that data. ANNs consist of several layers of interconnected nodes, or "neurons," which process information which can be passed on to the next layer. Each neuron in an ANN receives inputs from other neurons, applies a mathematical function to those inputs, and produces an output that is passed on to other neurons in the network. Through a process of trial and error, the network can learn to adjust the weights of the connections between neurons to improve its performance on a given task. Using ANN based maximum power point tracking MPPT model with interval type-2 fuzzy control, the wind generation can be optimized from the turbine to provide stable voltage to connected loads for the generator.

III. Control Procedure Adopted

A. ANN based controller

ANN is a technology adopted from the functional neural network. An artificial neuron is shown below in Fig.3. In Fig.3, the $x_1 \ldots x_n$ are the inputs to the neural network. The $w_1 \ldots w_n$ are the weights and y_o is the output. In the neural network used, the wind speed is used as the input to the neuron with each individual value of wind speed as the weights.

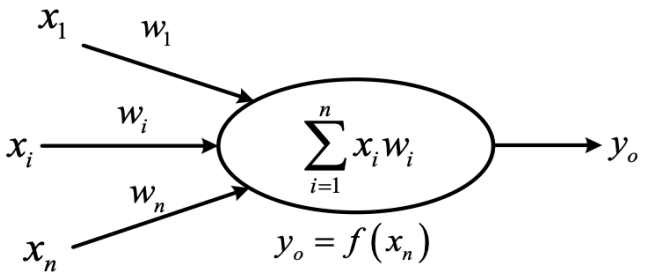

Fig.3. Artificial Neural Network (ANN) neuron.

ANN will predict the value of output to each value of wind speed. The output is the voltage value corresponding to the wind speed. The voltage output is predicted as a single layer ANN with wind speed as input. For extraction of maximum power, the MPPT used is designed with ANN and interval type-2 fuzzy logic. Here, after the output of ANN, interval type-2 fuzzy inference is used. For the wind turbine system, ANN is used to estimate the maximum output voltage value and interval type-2 fuzzy logic is used for generation of optimum duty cycle for pulses of the converter.

B. Interval Type-2 Fuzzy controller

A type-2 fuzzy inference ($\tilde{A}$) is characterized by its membership function $\mu_{\tilde{A}}(z,u)$ [20] as,

$$\tilde{A} = \int_{z \in Z} \int_{u \in J_z \subseteq [0,1]} \mu_{\tilde{A}}(z,u)/(z,u) \qquad (12)$$

wherein, z is a primary variable in Z universal set. The variable J_z is primary membership of z, with u as secondary variable. A secondary membership is also given and it is an upright slice of $\mu_{\tilde{A}}(z,u)$. There is a confined area within the primary and secondary functions which is the footprint of uncertainty (*FOU*).

The type-2 fuzzy sets involve large computations although they model the uncertainty in a better way than Type-1 fuzzy systems. If it is considered that for all values $\mu_{\tilde{A}}(z,u)=1$, the set converts into an interval type-2 fuzzy set. This reduces computations and complexity of the system as,

$$\tilde{A}=\int_{z\in Z}\left[\int_{u\in J_z\subseteq[0,1]}1/u\right]/z \qquad (13)$$

From (13), it is shown than the dimension is reduced which has homogeneous weighted primary membership values. The *FOU* or the bounded region is represented as,

$$\mathrm{FOU}(\tilde{A})=\bigcup_{z\in Z}J_z \qquad (14)$$

The type-2 Fuzzy inference system is shown in Fig.4 below.

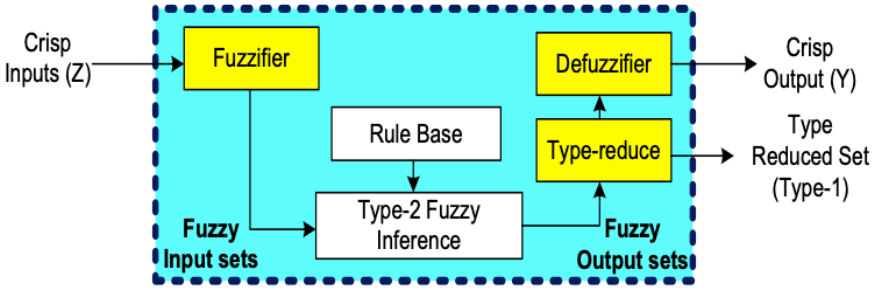

Fig.4. Type-2 Fuzzy Inference System.

This algorithm is used for designing the controller for providing the output pulses. These two combined controllers are used for designing the final MPPT for the wind turbine control. The combined controller design block diagram is shown in Fig.5. The control algorithms are used to design a program and used in the microcontroller device for controlling the wind turbine. The particulars are provided in the following Section IV of the paper.

doi.org/10.32388/D4GAVP.2

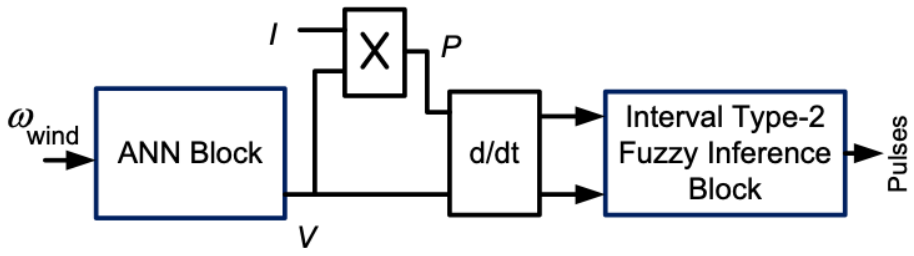

Fig.5. Combined controller for the bidirectional converter.

The interval type-2 based fuzzy controller generates the pulses for the bidirectional converter. The controller for the fuzzy interface has input membership function of derivative of power d*P* and voltage d*V*. The comparative error is taken as the switching function whose membership function is used in the interval type-2 fuzzy inference.

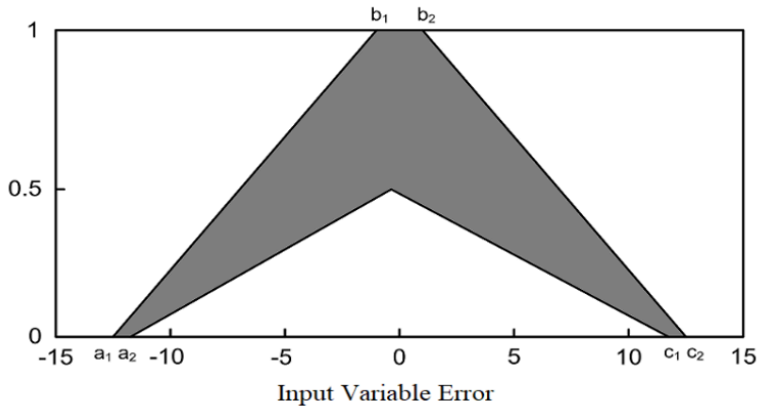

Fig.6. Membership function for input variable error.

The same is shown in Fig.6. Similar to type-1 fuzzy inference, interval type-2 fuzzy inference is represented using membership functions (MFs), with various ways to define shape or class of the set. Six parameter sets (a_1, a_2,..., c_2) are demarcated for interval type-2 fuzzy for the present problem like in [21].

C. Load Control

The three-phase fixed frequency inverter is used to supply the loads and it is driven at 50Hz frequency. The three-phase loads are connected using a smart electronic load controller. The controller is consisting

doi.org/10.32388/D4GAVP.2

of a relay-controlled switch which is controlled using an *Atmega* 328p controller (implemented using FANN (Fast Artificial Neural Network)). The smart electronic load controller is different from the conventional load controllers [22], [23] as it can also detect incipient faults besides controlling loads. Unbalanced loads [24] can also be detected. The controller takes the current data and is operated based on requirement and sensed load current. The smart controller is capable to sense faulty loads or loads with incipient fault using the sensed current. If there is a load with incipient fault, the load can be safely isolated also. Similar internet-of-things (IoT) based controllers are often used for load monitoring purposes [25], [26]. The smart controller is again configured using ANN based logic to obtain the ON/OFF control signals and its algorithm is shown. The controller hardware is shown in Fig.7.

Algorithm: Control of the connected loads.

1: $\forall j \in L$: read the ON/OFF status of individual loads.

2: $\forall ON_j \in L$: read power consumption using ANN logic.

3: $\forall ON_j \in L$: If, load power >> threshold, consider load turning OFF.
Else if, load power >> generated power, consider load turning OFF/ battery in discharging mode.
Else if, load power << generated power, load may remain ON/ battery in charging mode.

4: $\forall ON_j \in L$: calculate the value of V_j.

5: $V_j > \varepsilon$: load may have incipient fault and is isolated.

6: $\forall ON_j \in ON_\varepsilon$: load is turned OFF.

7: $\forall ON_j \notin ON_\varepsilon$: load can remain ON, go to 3.

8: Collect next time slot data, go to 1.

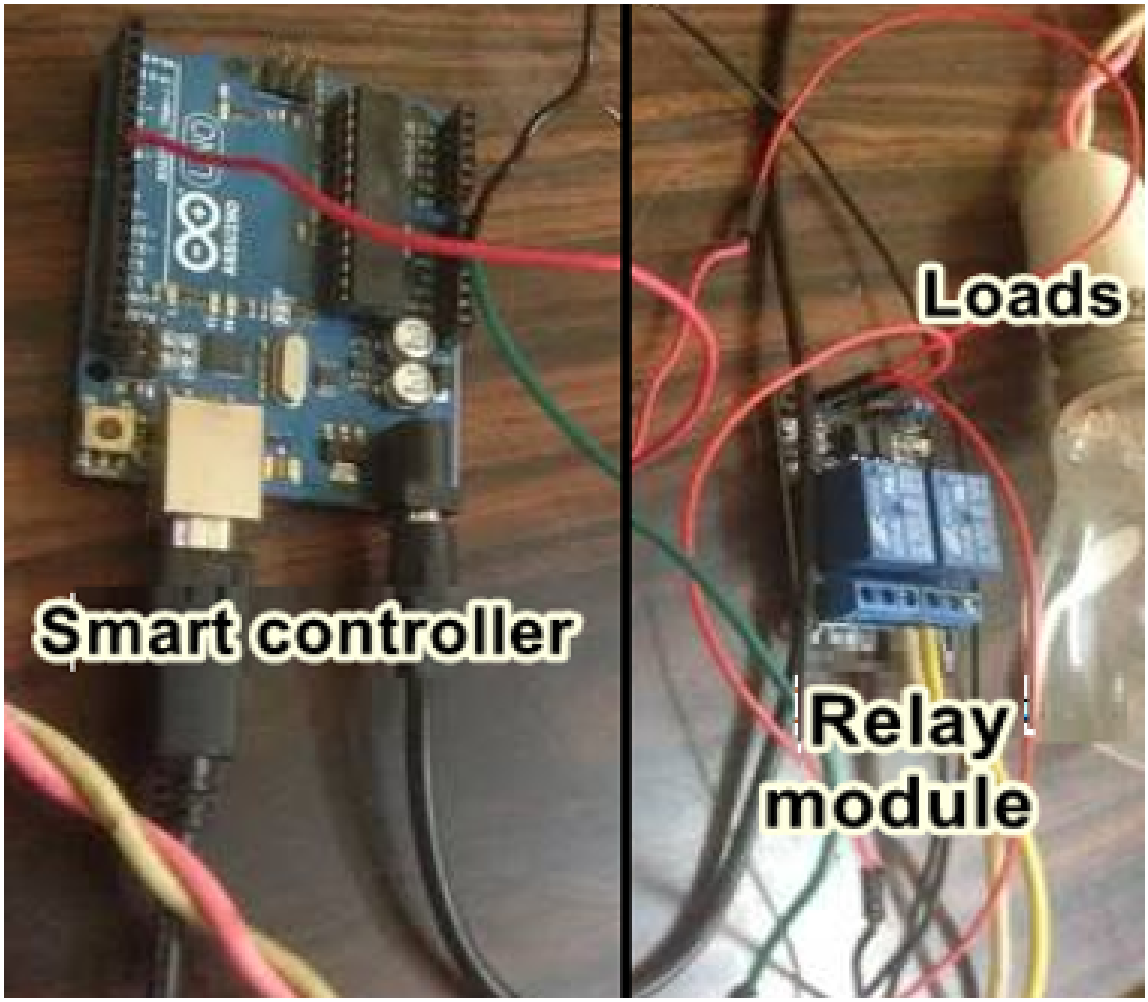

Fig.7. Smart controller with relay module for load control.

The ANN based load control is proposed which accounts for the control of domestic loads like ceiling fan and lights. It is done as follows:

i. Data collection: Data is collected for the usage of fan, light and other domestic loads. This data includes variables like time of day, temperature, and humidity (from capacitive humidity sensor).
ii. Data preparation: Collected data is preprocessed, including normalizing the values and splitting it into training and testing datasets.
iii. Building the neural network: Feedforward neural network architecture is used with a single hidden layer to train the model. The input layer has neurons for the collected variables, while the output layer has neurons for the control signals.

iv. Training the neural network: The neural network is trained using the training dataset. Backpropagation is used to adjust the weights and biases of the neurons to minimize the error between the predicted output and the actual output.

v. Testing the neural network: The testing dataset is used to evaluate the performance of the trained model.

The model is monitored for performance evaluation over time and is retrained it periodically using updated data if necessary. To enhance the model, additional layers or nodes to the neural network may also be added to include more input variables, or use a more advanced neural network architecture. Overall, the neural network architecture for controlling domestic loads like fans and lights using ANN is relatively simple feedforward architecture with a single hidden layer. The architecture for this task includes an input layer, a hidden layer, and an output layer. The input layer has neurons for the input variables, such as time of day, temperature, and humidity represented as s_1, s_2 s_3. The hidden layer has multiple neurons with nonlinear sigmoid activation function. The output layer has neurons for the control signals t_1 and t_2, to turn the fan and light ON/OFF. Each neuron in the hidden layer receives inputs from the input layer, which are weighted and summed, and then passed through a nonlinear activation function. The output of each hidden neuron is then weighted and summed to produce the final output of the network, which represents the control signals as shown in Fig.8.

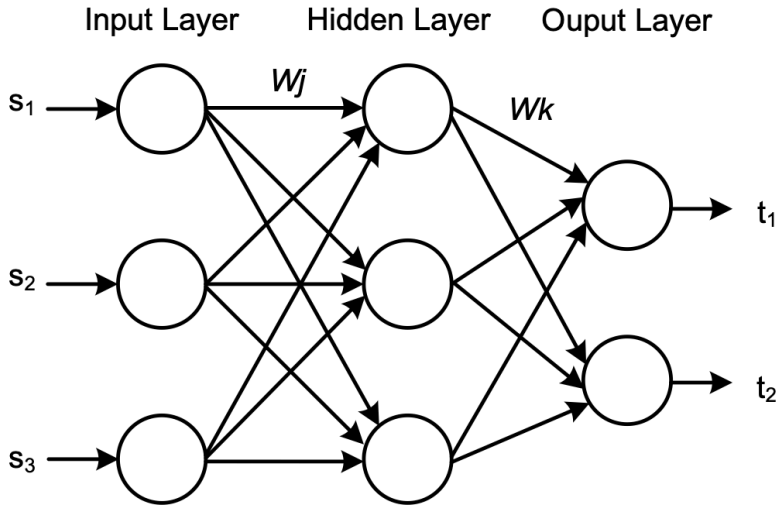

Fig.8. ANN structure for load control.

doi.org/10.32388/D4GAVP.2

The individual load powers are calculated and categorized for comparison and calculation of power requirement. All the loads are considered of ON/OFF type. The loads with incipient faults can be determined from the ON/OFF condition *K* of k^{th} no. of load and corresponding to its fundamental current signal *I*. The measured product value of the current and the ON/OFF condition and the stored product value is compared from (15). If the difference is significantly higher than a set threshold ε , the load may have incipient fault and needs to be isolated for further check.

$$V_j = \left[\sum_{z \neq j} I_k K_k(\text{ meas }) - \sum_{z \neq j} I_k K_k\right] \qquad (15)$$

IV. Simulation and Experimental Results

The proposed system is simulated using *MATLAB/Simulink* and the same system is also built as a laboratory prototype with turbine coupled three-phase induction generator.

A 1.5kW, 400V, 50Hz, 4-pole, three-phase, cage rotor induction machine is used as induction generator for laboratory experimental purposes. Wind turbine is chosen at 2kW with scaled annual average wind speed of 5m/s. The terminal capacitor bank used is of 30µF connected in delta and is obtained by reactive power balancing following [27] of the machine at no-load condition. The bidirectional converter uses MOSFETS, K2611 with 900V, 11A ratings. The MOSFETS are driven by dedicated gate driver circuits using *ATMEGA* microcontroller. The other inverter is operated at a fixed frequency of 50Hz for maintaining fixed frequency voltage at the load terminals. Rechargeable lead-acid battery unit of 77Ah, 48V is used with its inherent charge controller. The system load is rated at 1.1kW at 0.8 *p.f.* lagging.

The induction generator with the proposed control is studied for no-load and rated load conditions. With the proposed control, the induction generator shows stable terminal voltage at no-load and at rated load than without the proposed control technique as shown in Fig.9.

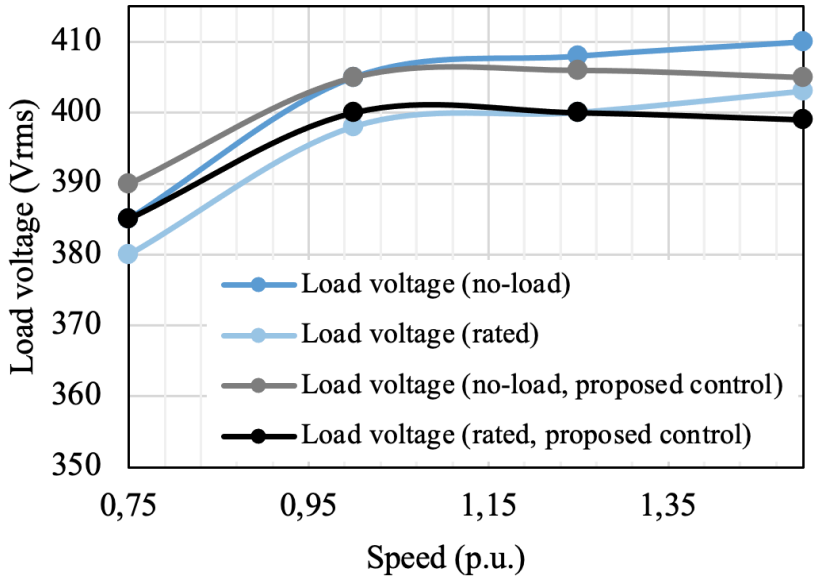

Fig.9. Plot showing generated voltage variation with change in speed.

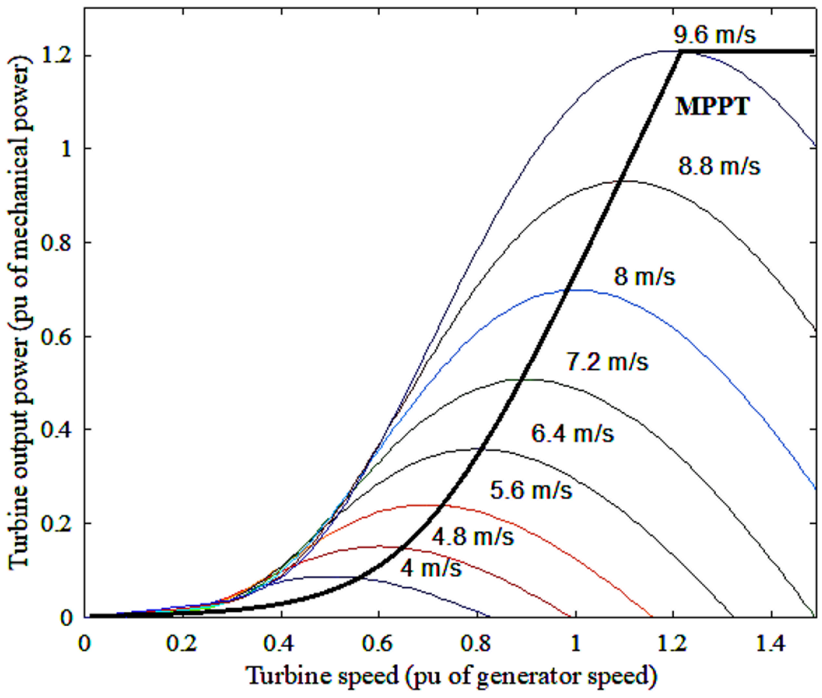

Fig.10. Plot showing the turbine power curves along with MPPT (bold black line).

doi.org/10.32388/D4GAVP.2

A simulation study is carried out using *MATLAB/Simulink* platform for simulating the proposed generation with its control. The induction generator model uses the same parameters as that of the experimental machine. The simulations are run on a Windows 11 enabled system with Core i5, 8^{th} Gen. processor. The simulated model uses a bidirectional converter and storage battery assembly connected to the DC bus. In the simulation study, a wind turbine model is used whose power curve characteristics is shown in Fig.10.

The simulated model is then tested for voltage build-up and proposed control with load and speed variations. The simulated results are then compared with the experimental results obtained from the tests. As observed, the experimental results are in good agreement with the simulated model of the generation scheme.

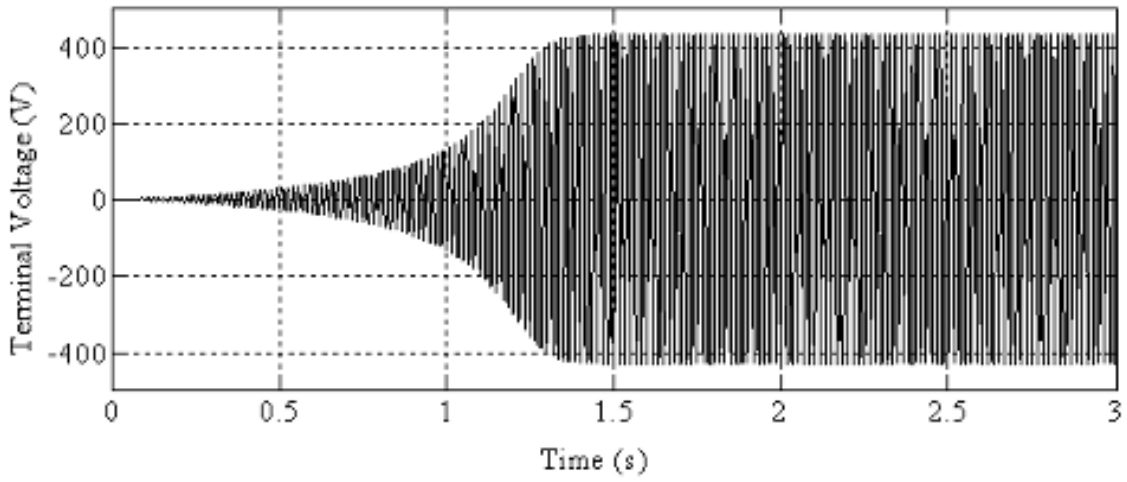

Fig.11. Simulated waveform for terminal voltage build-up of generator.

doi.org/10.32388/D4GAVP.2

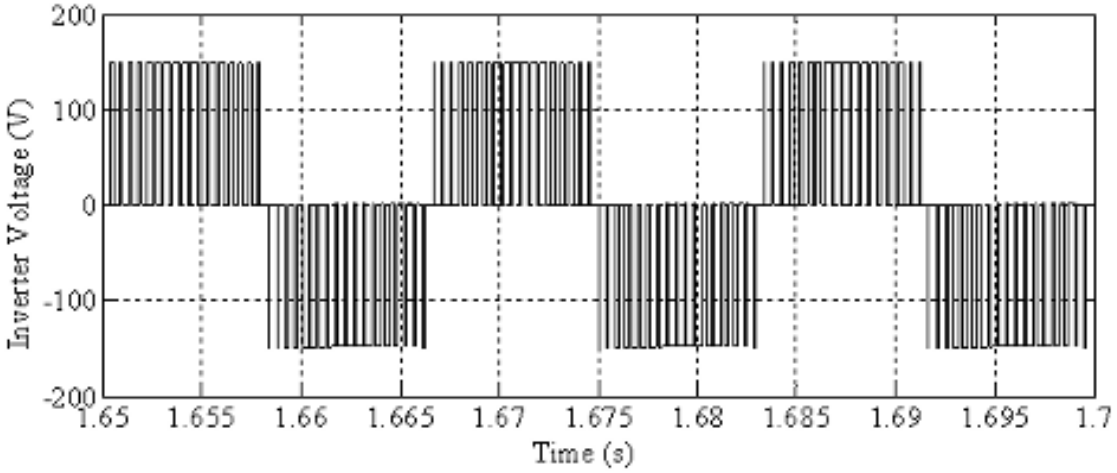

Fig.12. Simulated waveform for bidirectional converter output voltage.

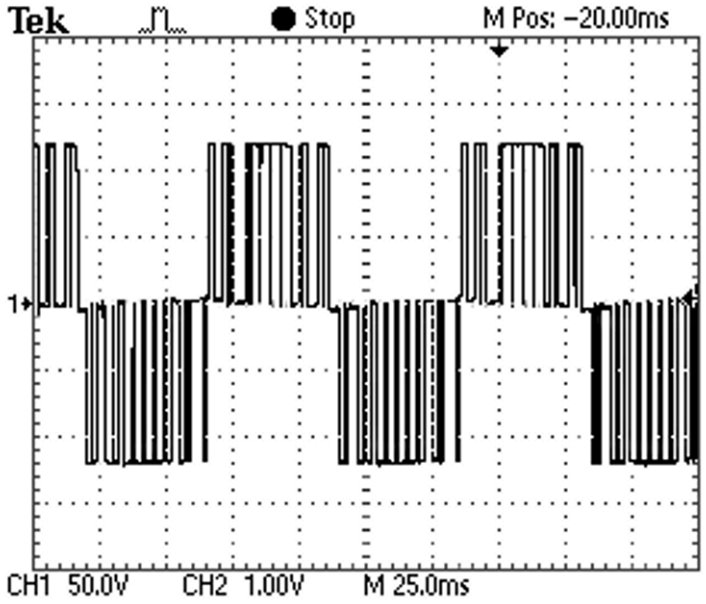

Fig.13. Experimental waveform for inverter output voltage (CH1, 50V/div.).

The results are in good agreement as seen from the plots. Fig.11 shows the simulated generator terminal voltage build-up waveform and Fig.12 shows the waveform for the bidirectional converter working in inverting mode respectively. The experimental bidirectional converter output voltage waveform is shown

doi.org/10.32388/D4GAVP.2

in Fig.13. Fig.14(a) shows the simulation waveform for the load current when load is varied from 1A to 2A peak current. The corresponding voltage waveform is shown in Fig.14(b). It is also observed that with 50% increase in load current, the load voltage change is almost insignificant. The same verification is done experimentally using the experimental setup.

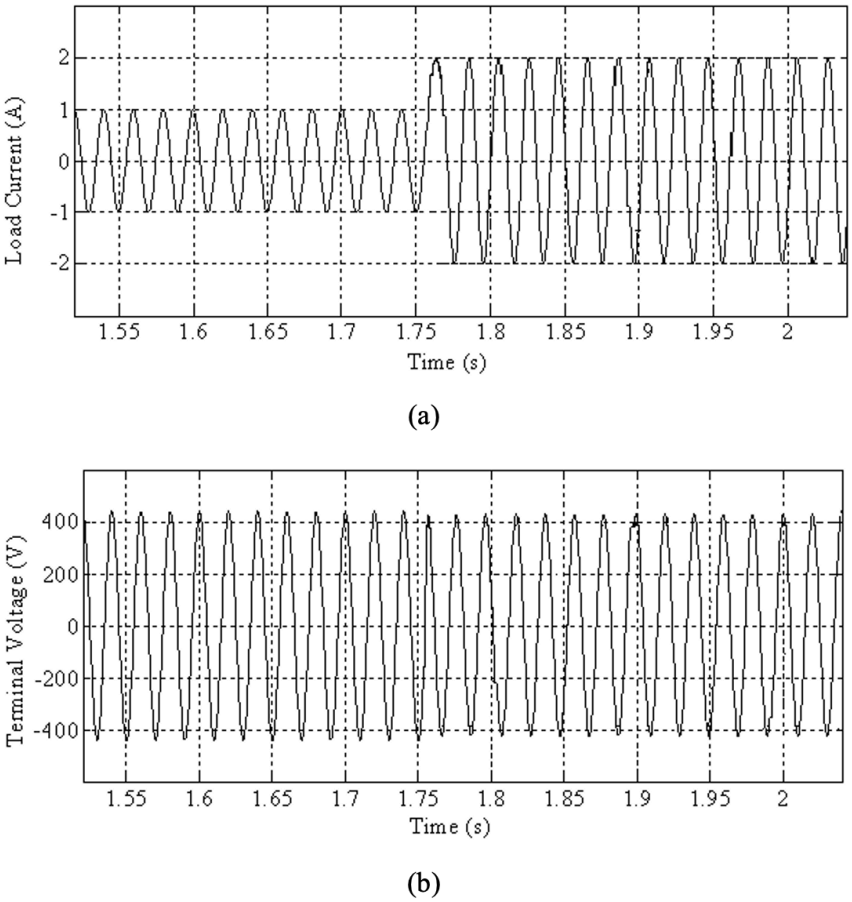

Fig.14. Waveform for variation of (a) load current and its (b) corresponding terminal voltage.

Fig.15 shows the experimental waveform of the load current and terminal voltage when same variation of load is done as in case of simulation performed. The results as shown are in good agreement with the observed simulation results.

doi.org/10.32388/D4GAVP.2

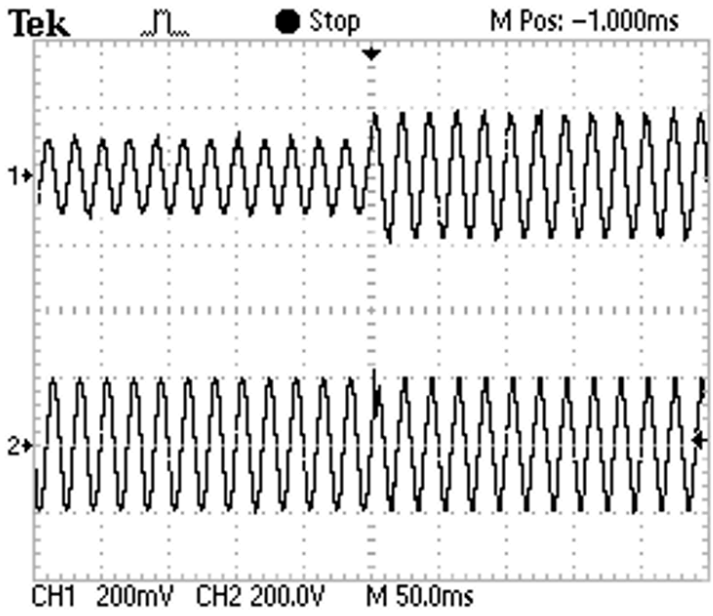

Fig.15. Experimental waveform for load current (CH1, 2A/div.) and terminal voltage (CH2, 400V/div.).

Fig.16 shows the detection of incipient faults for the loads. For the proposed scheme, different loads like LED lights and ceiling fans are used. The loads are run for 5 hours and their *Vj* signatures are noted using (15). As observed from the Fig.16, the Fan 2 load value for the same is lower than the set tolerance value after 3rd hour and it remains same for the rest of the considered time. This indicates that the fan load may have some incipient fault. This load is then isolated for further study of its likely fault. On contrary, the Fan 3 load has reached zero value indicating the load is turned OFF at t = 4hrs.

doi.org/10.32388/D4GAVP.2

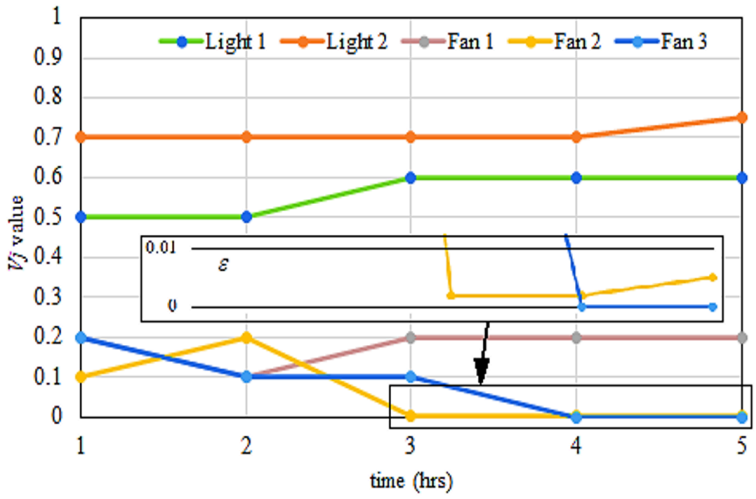

Fig.16. Load fault detection using the proposed scheme.

A qualitative comparisonal analysis is done for the proposed scheme with similar state-of-the-art generating schemes as given in Table I. The comparison is done based on the effectiveness of the different control schemes adopted in recent times for wind power generation and control. The parameters used for the comparison are, the difficulty in implementation due to either complex control or components used, MPPT based power utilization, short time load voltage transients observed and load control availability. For the proposed control, the implementation difficulty is minimal with minimal hardware components used than rest of the schemes compared with. Also, the MPPT based wind power utilization using ANN and interval type-2 controller is unique and better for grid-secluded generations. Short time load voltage transients are minimized and hence voltage regulation is better for the proposed scheme. Another advantage of the proposed scheme is the smart load control with incipient fault detection which is a new feature unlike previously adopted electronic load controllers using dump loads [7].

doi.org/10.32388/D4GAVP.2

Reference, year	Implementation difficulty	MPPT based wind power utilization	Short time voltage transients	Smart load control
[9], 2017	Yes	Yes	No	No
[14], 2020	Yes	Yes	Minimal	No
[10], 2022	Minimal	No	Yes	Yes
Proposed	No	Yes	No	Yes

Table I. Comparison with Similar Wind Generation Schemes

Quantitative analysis could not be done as most of the available techniques are having different system ratings or varying system configurations and hence all assumptions are avoided. In [9], a MPPT approach is used for wind turbine control wherein similar turbine is adopted. Control complexity is similar with identical implementation hardware requirement. However, the proposed MPPT can adapt to rapidly changing wind conditions which is not possible in [9] and hence a dynamic voltage controller is also adopted for the generator along with the MPPT control.

The simulated reliability of the proposed scheme is also studied. Though various probability indices may be calculated, loss of load expectation (*LOLE*) [28] is considered, which calculates the time period that the system is not capable to supply the loads and it is given as,

$$LOLE = \sum_{i=1}^{n} t_i \left(P_{Gi} < P_{Li}\right) \qquad (16)$$

where, *i*, *n*, P_{Gi}, P_{Li} and t_i are the sampling interval, total samples, generated power, and load power and total time when load is not supplied respectively. The reliability is calculated using two scenarios as shown in Table II. An annual simulation sampling of 5340 hours is made, considering the renewable generation using proposed MPPT, the load demand and the storage battery characteristics. The lesser the index value, the better is the reliability and as observed, the Case II with the proposed sources provide better results.

Cases of generation with proposed MPPT	*LOLE (h)*
I. Wind generation alone	157
II Wind and storage battery (present scheme)	73

Table II. Values of Reliability Index

V. Conclusion

An induction generator-based generation scheme is proposed with an ANN and interval type-2 fuzzy inference-based MPPT control. The loads can also be operated and controlled based on the proposed scheme. The generation scheme can be easily fabricated in remote and grid isolated areas with a wind turbine for grid-secluded microgeneration applications. The proposed control strategy effectively overcomes the problem of voltage regulation during load or wind speed perturbations. A smart ANN based load control is also proposed which can effectively detect incipient load faults. A comparison drawn between similar schemes illustrate the superiority of the proposed scheme for grid-isolated generation with better reliability as regards power availability.

In future, the generation scheme can be extended for its connection with a grid and further, improved control strategies can be implemented for wider wind speed range utilization and for further minimization of wind sand load transients.

References

1. ^*M. R Patel and O. Beik. "Wind and Solar Power Systems", 3rd edn., CRC Press, UK, 2021.*
2. ^*H. Chojaa et al., "A novel DPC approach for DFIG-based variable speed wind power systems using dspace," IEEE Access, vol. 11, pp. 9493-9510, 2023.*
3. ^*H. Chojaa et al., "Advanced control techniques for doubly-fed induction generators based wind energy con version systems," 2022 Global Energy Conf. (GEC), Batman, Turkey, 2022, pp.282-287, doi: 10.1109/GEC5501 4.2022.9987088.*
4. ^a, ^b*C. P. Ion, "A comprehensive overview of single–phase self-excited induction generators," IEEE Access, vol. 8, pp. 197420-197430, 2020.*

5. ^M. Faisal Khan, M. R. Khan, A. Iqbal, “Effects of induction machine parameters on its performance as a sta ndalone self excited induction generator,” Energy Reports, vol.8, p. 2302, 2022.
6. ^V. B Murali Krishna, V. Sandeep, SS Murthy and K. Yadlapati “Experimental investigations on performance comparison of self excited induction generator and permanent magnet synchronous generator for small sc ale renewable applications,” Renew. Energy, vol. 195, pp. 431-441, Aug. 2022.
7. a, bI. Grgić, M. Bašić, D. Vukadinović and M. Bubalo, “Optimal control of a standalone wind-solar-battery po wer system with a quasi-z-source inverter,” 2020 9th Int. Conf. Renewable Energy Research and Application (ICRERA), Glasgow, UK, 2020, pp. 61-66, doi: 10.1109/ICRERA49962.2020.9242854.
8. ^S. Stanković, T. Van Cutsem and L. Söder, “Fault-current injection strategies of inverter-based generation f or fast voltage recovery,” IEEE Trans. Pow. Syst., vol. 37, no. 2, pp. 1543-1553, March 2022.
9. a, b, c, dV. K. Murali and V. Sandeep, “Design and simulation of current sensor based electronic load controlle r for small scale three phase self excited induction generator system”, Int. J. Renew. Energy Res., vol. 10, no. 4, pp. 1638- 1644, Dec. 2020.
10. a, bA.Chatterjee, and D. Chatterjee, “PV-assisted microgeneration scheme with single-phase induction gener ator suitable for wide speed range application,” IET Power Electron., vol. 10, no. 14, pp. 1859-1869, 2017.
11. ^H. Shutari, T. Ibrahim, N. B. Mohd Nor, N. Saad, M. F. N. Tajuddin and H. Q. A. Abdulrab, “Development of a novel efficient maximum power extraction technique for grid-tied VSWT system,” IEEE Access, vol. 10, pp. 1 01922-101935, 2022.
12. ^B. Hamid, I. Hussain, S. J. Iqbal, B. Singh, S. Das and N. Kumar, “Optimal MPPT and BES control for grid-tie d DFIG-based wind energy conversion system,” IEEE Trans. Ind. Appl., vol. 58, no. 6, pp. 7966-7977, Nov.-Dec. 2022.
13. ^P. Huynh, S. Tungare and A. Banerjee, “Maximum power point tracking for wind turbine using integrated generator–rectifier systems,” IEEE Trans. Pow. Electron., vol. 36, no. 1, pp. 504-512, Jan. 2021.
14. a, bA. Chatterjee, “Wind-PV based generation with smart control suitable for grid-isolated critical loads in o nshore India,” J. Inst. Eng. India Ser. B, 2022. https://doi.org/10.1007/s40031-022-00827-2.
15. ^A. Chatterjee, S. Ghosh and A. Mitra, “Wind-PV based isolated hybrid generation for smart irrigation man agement and supplying other critical loads,” IEEE 2nd Int. Conf. Sust. Energy Future Electric Transp. (SeFe T), pp. 1-6, 2022.
16. a, bB. K. Bose, Modern power electronics and AC drives, Prentice Hall PTR, New Jersey, USA, 2001.
17. ^R. Lippmann, “An introduction to computing with neural nets,” IEEE ASSP Magazine, vol. 4, no. 2, pp. 4-22, Apr 1987, doi: 10.1109/MASSP.1987.1165576.

18. ^ *N. Kumar and G. Dyanamina, "Performance improvement of SEIG based WECS using artificial neural net work," 2023 IEEE International Students' Conference on Electrical, Electronics and Computer Science (SCEE CS), Bhopal, India, pp. 1-6, 2023.*
19. ^ *H. Elaissaoui, M. Zerouali, A. E. Ougli and B. Tidhaf, "MPPT algorithm based on fuzzy logic and artificial n eural network (ANN) for a hybrid solar/wind power generation system," 2020 Fourth Int. Conf. Intel. Comp. Data Sciences (ICDS), Fez, Morocco, 2020, pp. 1-6.*
20. ^ *S. Ghosh, A. Chatterjee, and D. Chatterjee, "Extraction of statistical features for type-2 fuzzy NILM with IoT enabled control in a smart home," Expert Syst. Appl., vol. 212, p.118750, 2023.*
21. ^ *K. Mittal, A. Jain, K. S. Vaisla, O. Castillo, and J. Kacprzyk, "A comprehensive review on type 2 fuzzy logic ap plications: Past, present and future," Eng. Appl. Artif. Intell., vol. 95, p. 103916, 2020.*
22. ^ *B. Singh, S. S. Murthy and S. Gupta, "Transient analysis of self-excited induction generator with electronic l oad controller (ELC) supplying static and dynamic loads," IEEE Trans. Ind. Appl., vol. 41, no. 5, pp. 1194-1204, Sept.-Oct. 2005.*
23. ^ *B. N. Roodsari and E. P. Nowicki, "Analysis and experimental investigation of the improved distributed elec tronic load controller," IEEE Trans. Energy Conv., vol. 33, no. 3, pp. 905-914, Sept. 2018.*
24. ^ *A. Chatterjee and D. Chatterjee, "An improved current balancing technique of two-winding IG suitable for wind-pv-based grid-isolated hybrid generation system," IEEE Syst. J., vol. 14, no. 4, pp. 4874-4882, Dec. 202 0.*
25. ^ *S. Ghosh, A. Chatterjee and D. Chatterjee, "Load monitoring of residential elecrical loads based on switchi ng transient analysis," 2017 IEEE Calcutta Conf. (CALCON), Kolkata, India, pp. 428-432, 2017.*
26. ^ *S. Ghosh, A. Chatterjee and D. Chatterjee, "A smart IoT based non-intrusive appliances identification techn ique in a residential system," 2020 IEEE Int. Conf. Pow. Electron., Smart Grid Renew. Energy (PESGRE2020), Cochin, India, pp. 1-6, 2020.*
27. ^ *A.M. Trzynadlowski, "Control of Induction Motors", 1st edn., Academic Press, USA, 2001.*
28. ^ *W. Ahmad, O. Hasan, F. Awwad, N. Bastaki and S. R. Hasan, "Formal reliability analysis of an integrated po wer generation system using theorem proving," IEEE Syst. J., vol. 14, no. 4, pp. 4820-4831, Dec. 2020.*

Declarations

Funding: No specific funding was received for this work.

Potential competing interests: No potential competing interests to declare.